Guided Ion Beam Studies of the Reactions of Group 3 Metal Ions (Sc^+, Y^+, La^+, and Lu^+) with Silane. Electronic State Effects, Comparison to Reactions with Methane, and M^+-SiH_x ($x = 0-3$) Bond Energies

Bernice L. Kickel and P. B. Armentrout*

Contribution from the Department of Chemistry, University of Utah, Salt Lake City, Utah 84112

Received October 6, 1994®

Abstract: Guided ion beam techniques are used to measure cross sections as a function of kinetic energy for the reactions of silane with $M^+ = Sc^+$, Y^+, La^+, and Lu^+. Ionic products include MH^+ and MH_2^+, as well as $MSiH_x^+$ ($x = 0-3$). The major low-energy process in all four systems is formation of $MSiH_2^+ + H_2$, while at higher energies, formation of $MH^+ + SiH_3$ and $MH_2^+ + SiH_2$ dominates the reactivity. Variation of source conditions allows the effect of electronic excitation on the reactivity of Sc^+ and Y^+ to be studied in detail. The Sc^+ (a^3D) ground state and the Y^+ (a^3D) first excited state are approximately an order of magnitude less reactive than the Sc^+ (a^1D, a^3F) excited and the Y^+ (a^1S) ground states. Formation of $ScH_2^+ + SiH_2$ is observed only for reaction of silane with Sc^+ (a^1D). The reactivity of these systems may be understood in terms of simple molecular orbital and spin conservation concepts. The thresholds for Sc^+, Y^+, La^+, and Lu^+ reactions are evaluated to yield 0 K bond dissociation energies (BDEs) for M^+-Si, M^+-SiH, M^+-SiH_2, and M^+-SiH_3 of 2.51 ± 0.11, 2.33 ± 0.11, 2.17 ± 0.08, and 1.76 ± 0.16 eV, respectively, for M = Sc; 2.52 ± 0.13, 2.82 ± 0.16, ≥2.39 ± 0.07, and 2.13 ± 0.16 eV, respectively, for M = Y; and 2.87 ± 0.10, 2.76 ± 0.25, ≥2.39 ± 0.07, and 2.00 ± 0.28 eV, respectively, for M = La. In the case of Lu^+, the M^+-Si and M^+-SiH_2 BDEs are 1.11 ± 0.14 and 0.98 ± 0.10 eV, respectively. Values determined in the present study for $D_0(M^+ - H)$ and $D_0(M^+-2H)$ on the basis of state-specific information indicate that a reexamination of previously determined values may be warranted.

Introduction

Over the past 30 years, interest in transition-metal−silicon bonded compounds in the condensed phase has grown steadily.[1] This interest has been prompted by the discovery of transition-metal-complex catalyzed hydrosilation.[2] More recently, attention has focused on the role played by these complexes in silane polymerization[3] and the catalysis in chemical vapor deposition (CVD) of silicones[4] and of transition-metal silicides.[5] These processes can be quite complex and fundamental information regarding possible transition-metal−silicon intermediates would be useful in understanding their reactivity. Although some information regarding these species is available in the condensed phase, there is no thermodynamic data and relatively little is known about these species in the gas phase. To provide such fundamental information, we have begun a series of experiments designed to examine the gas-phase reactivity of atomic transition-metal ions with silane.[6-8]

Previous experimental work of relevance to the title systems includes studies of Geribaldi and co-workers,[9] who utilized Fourier-transform ion cyclotron resonance (FTICR) mass spectrometry to investigate the reactions of Sc^+, Y^+, and Lu^+ with silane. They found the reaction with Y^+ to form $YSiH_2^+$ to be rapid and exothermic, while the reactivity with Lu^+, even if translationally activated, was negligible. Reaction of translationally activated Sc^+ with silane was observed to be slow and endothermic and led first to the formation of $ScSiH_2^+$ and ScH^+. The latter product then reacted with SiH_4 to form $ScSiH_3^+ + H_2$. They also observed hydride abstraction (formation of $SiH_3^+ + ScH$) for translationally activated Sc^+. At high pressures of silane, oligomerization reactions yielding $MSi_nH_{2n}^+$ and $MSi_nH_{2n-2}^+$ up to $n = 3$ for M = Sc and $n = 7$ for M = Y, and $ScSi_nH_{2n-4}^+$ and $ScSi_n^+$ up to $n = 3$. Because Geribaldi and co-workers generate the Sc^+, Y^+, and Lu^+ metal ions by nitrogen-laser ablation of metal targets, a method that often leads to production of excited state metal ions, it is unclear from these studies how the electronic states influence the periodic trends observed in the chemistry.

In addition to this experimental study, Cundari and Gordon have completed theoretical calculations to investigate the nature of bonding in simple first-row transition-metal−silylene ions, $MSiH_2^+$, where M = Sc to Ni.[10] For comparison, they also investigated first-row transition-metal−carbene complexes, MCH_2^+. Musaev et al. calculate similar comparisons down the group 9 series (M = Co, Rh, and Ir).[11] Both groups find that the silylene complexes have weak bonds compared to their MCH_2^+ counterparts and other multiply bonded species. Of particular interest is theoretical work by Ferhati and Ohanessian, who have calculated the potential energy surfaces for the

® Abstract published in *Advance ACS Abstracts,* March 15, 1995.

(1) Tilley, T. D. *The Chemistry of Organic Silicon Compounds*; Wiley: New York, 1989; Chapter 24.

(2) Speier, J. L.; Webster, J. A.; Barnes, G. H. *J. Am. Chem. Soc.* **1957**, *79*, 974.

(3) Harrod, J. F.; Ziegler, T.; Tschinke, V. *Organometallics* **1990**, *9*, 897. Tilley, T. D.; Woo, H. G. *J. Am. Chem. Soc.* **1989**, *111*, 8043.

(4) Ensslen, K.; Veprek, S. *Plasma Chem. Plasma Proc.* **1987**, *7*, 139.

(5) Corey, J. Y.; Corey, E. R.; Gaspar, P. P., Eds. *Silicon Chemistry*; Horwood: Chichester, 1988.

(6) Kickel, B. L.; Armentrout, P. B. *J. Am. Chem. Soc.* **1994**, *116*, 10742.

(7) Kickel, B. L.; Armentrout, P. B. *J. Am. Chem. Soc.* **1995**, *117*, 764.

(8) Kickel, B. L.; Armentrout, P. B. *J. Phys. Chem.* **1995**, *99*, 2024.

(9) Decouzon, M.; Gal, J.-F.; Geribaldi, S.; Rouillard, M.; Sturla, J.-M. *Rapid Comm. Mass Spectrom.* **1989**, *3*, 298. Azzaro, M.; Breton, M.; Decouzon, M.; Geribaldi, S. *Rapid Comm. Mass Spectrom.* **1992**, *6*, 306.

(10) Cundari, T. R.; Gordon, M. S. *J. Phys. Chem.* **1992**, *96*, 631.

(11) Musaev, D. G.; Morokuma, K.; Koga, N. *J. Chem. Phys.* **1993**, *99*, 7859.

0002-7863/95/1517-4057$09.00/0

reaction of Y^+ with silane and investigated a number of possible reaction pathways and intermediates.[12]

In the present study, we extend the work of Geribaldi and co-workers[9] by using guided ion beam mass spectrometry to measure the kinetic energy dependence of the reactions of silane with Sc^+, Y^+, La^+, and Lu^+. Variation of the ion source conditions allows us to explicitly examine contributions of excited states of Sc^+ and Y^+ to the observed reactivity. Where possible, the kinetic energy dependence of the cross sections is analyzed to yield M^+-SiH_x ($x = 0-3$) bond energies. Thermodynamic and state-specific results are combined to provide information regarding likely reaction mechanisms. Trends in metal−silicon thermochemistry are discussed in terms of a comparison to silicon−silicon bonded analogues. The results of these reactions are also compared with the previously studied reactions of methane with Sc^+, Y^+, La^+, and Lu^+.[13]

Experimental Section

General. A complete description of the apparatus and experimental procedures is given elsewhere.[14,15] Briefly, ions are produced as described below, accelerated, and focused into a magnetic sector momentum analyzer for mass analysis. They are then decelerated to the desired translational energy and focused into an octopole ion beam guide[16] that traps ions in the radial direction. The octopole passes through a static gas cell containing a low pressure (0.03−0.1 mTorr) of the SiH_4 reactant, such that multiple ion−molecule collisions are improbable. Pressure-dependent studies verify that the cross sections shown below are due to single ion−molecule collisions. After exiting the reaction cell, the ions are extracted from the octopole, focused into a quadrupole mass filter for mass analysis, and detected by using a scintillation ion detector and standard ion counting techniques. Raw ion intensities are converted into absolute reaction cross sections with estimated uncertainties of ±20% and relative uncertainties of ±5%.[14]

Laboratory ion energies (lab) are converted to energies in the center-of-mass frame (CM) by using $E_{CM} = E_{Lab}M/(m + M)$, where m is the mass of the metal ion and M is the isotopically averaged mass of SiH_4. Unless stated otherwise, all energies quoted in this work correspond to the CM frame. The absolute energy and the energy distribution of the ions in the interaction region are measured by using the octopole as a retarding field analyzer.[14] The uncertainty in the absolute energy scale is ±0.05 eV (lab). The distribution of ion energies has an average full width at half-maximum (fwhm) of ~0.4 eV (lab). The thermal motion of the gas in the reaction cell has a distribution with a fwhm of $\sim 0.4E_{CM}^{1/2}$ (eV).[17] At very low energies, the slower ions in the kinetic energy distribution of the beam are not transmitted through the octopole, resulting in a narrowing of the ion energy distribution. We take advantage of this effect to access very low interaction energies as described previously.[14,18]

Ion Source. A dc-discharge flow tube (DC/FT) ion source, described in detail previously,[15] is used to form Sc^+, Y^+, La^+, and Lu^+ ions. The dc-discharge is used to ionize and accelerate argon ions into scandium metal or $MCl_3 \cdot 7H_2O$ (where M = Y, La, and Lu) to sputter off the desired atomic metal ion. Attempts to use $ScCl_3 \cdot 7H_2O$ in the DC/FT resulted in contamination of the Sc^+ ion beam that interfered with the present experiment. The resulting ions are swept downstream in a flow of helium and argon at a total pressure of 0.4−0.7 Torr and encounter $> 10^5$ collisions with the bath gas. It is believed that most excited states of Sc^+, Y^+, La^+, and Lu^+ are quenched to their ground states by these collisions. However, we do observe indications of a small amount of Lu^+ (a^3D) excited state, which could account for as little as 0.10% of the beam (see below). This is easily accounted for in the cross sections measured here.

Table 1. Electronic States of Sc^+, Y^+, La^+, and Lu^+

				% population	
M^+	state	config	energy,[a] eV	300 K[b]	2250 K[c]
Sc^+ [d]	a^3D	$4s3d$	0.013	99.99	88.1
	a^1D	$4s3d$	0.315	0.01	6.2
	a^3F	$3d^2$	0.608		5.7
	b^1D	$3d^2$	1.357		<0.1
Y^+ [e]	a^1S	$5s^2$	0.000	91.5	11.4
	a^3D	$5s4d$	0.148	8.5	80.6
	a^1D	$5s4d$	0.409		6.9
	a^3F	$4d^2$	1.045		1.1
	a^3P	$4d^2$	1.742		≪0.1
La^+ [f]	a^3F	$5d^2$	0.147	99.9	68.9
	a^1D	$6s5d$	0.173	0.1	12.6
	a^3D	$6s5d$	0.342	<0.1	16.7
	a^3P	$5d^2$	0.738		1.3
	a^1S	$6s^2$	0.917		0.1
	a^1G	$5d^2$	0.927		0.5
	b^1D	$5d^2$	1.252		<0.1
Lu^+ [f]	a^1S	$6s^2$	0.000	100	99.6
	a^3D	$6s5d$	1.628		0.4
	a^1D	$6s5d$	2.149		<0.1

[a] Energies are a statistical average over the J levels. [b] 400 K for Sc^+. Maxwell−Boltzmann distribution at this temperature, which is associated with the DC/FT source for Sc^+ and Y^+, and possibly La^+ and Lu^+. [c] Maxwell−Boltzmann distribution at 2250 K, the temperature of the surface ionization filament. [d] Values from: Sugar, J.; Corliss, C. *J. Phys. Chem. Ref. Data* **1980**, *9*, 473−511. [e] Reference 25. [f] Reference 26.

Ion beams of Sc^+, Y^+, La^+, and Lu^+ were also produced in a surface ionization (SI) source. Here, the metal is introduced to the gas phase by vaporizing MCl_3 (where M = Sc, Y, La, Lu) in an oven. The metal-containing vapor is passed over a resisitively heated rhenium filament at a temperature in the range of 2000 to 2300 ± 100 K, as measured by optical pyrometry. Dissociation of the metal halides and ionization of the resultant metal atoms occurs on the filament. We assume that a Maxwell−Boltzman distribution accurately describes the populations of the electronic states of Sc^+, Y^+, La^+, and Lu^+. The validity of this assumption has been discussed previously,[19] and work by van Koppen *et al.* has verified this assumption in the case of Co^+.[20]

The metal chlorides are obtained from Aesar and are used without further purification. The SiH_4 was of semiconductor purity and obtained from Matheson Gas Products.

Thermochemical Analysis. The threshold regions of the experimental reaction cross sections are analyzed by using the empirical model in eq 1.

$$\sigma(E) = \sigma_0 \sum g_i (E + E_{rot} + E_i - E_0)^n / E \qquad (1)$$

Here, E is the relative kinetic energy, E_0 is the reaction endothermicity for reaction of the lowest J state of the ion at 0 K, σ_0 is an energy-independent scaling factor, and n is an adjustable parameter. This equation takes the internal energy of the SiH_4 reagent into consideration by including the average rotational energy, $E_{rot}(SiH_4) = 3kT/2 = 0.039$ eV at 300 K. Vibrational energy contributions are negligible (<0.007 eV). The summation is over the distribution of electronic states i of the metal ion reactant having energies E_i (Table 1 gives J-averaged values) and relative populations g_i, where $\sum g_i = 1$. The resulting model cross section is then convoluted with the ion and neutral translational energy distributions before comparison with the data. The parameters n, σ_0, and E_0 are allowed to vary freely to best fit the data as determined by a nonlinear least-squares analysis. For analyses of some small cross sections, it was necessary to fix the value of n over an acceptable range while allowing σ_0 and E_0 to vary freely. It is possible that this could introduce systematic errors in the thresholds determined, but the range of n values chosen in each case is large enough to include all likely

(12) Ferhati, A. Ph.D. Thesis, Universite de Paris-Sud, 1994. Ohanessian, G., personal communication, 1994.
(13) Sunderlin, L. S.; Armentrout, P. B. *J. Am. Chem. Soc.* **1989**, *111*, 3845.
(14) Ervin, K. M.; Armentrout, P. B. *J. Chem. Phys.* **1985**, *83*, 166.
(15) Schultz, R. H.; Armentrout, P. B. *Int. J. Mass Spectrom. Ion Processes* **1991**, *107*, 29.
(16) Teloy, E.; Gerlich, D. *Chem. Phys.* **1974**, *4*, 417.
(17) Chantry, P. J. *J. Chem. Phys.* **1971**, *55*, 2746.
(18) Ervin, K. M.; Armentrout, P. B. *J. Chem. Phys.* **1987**, *86*, 2659.
(19) Sunderlin, L. S.; Armentrout, P. B. *J. Phys. Chem.* **1988**, *92*, 1209.
(20) van Koppen, P. A. M.; Kemper, P. R.; Bowers, M. T. *J. Am. Chem. Soc.* **1992**, *114*, 10941.

Table 2. Heats of Formation and Ionization Energies at 0 K

species	$\Delta_f H_0$, eV	IE, eV
H	2.239[a]	
SiH_4	0.46 (0.02)[a]	
SiH_3	2.14 (0.03)[b]	8.135 (0.005)[c]
SiH_2	2.85 (0.07)[d]	
SiH	3.92 (0.04)[e]	
Si	4.66 (0.03)[f]	
ScH		6.2 (0.2)[g]

[a] Reference 52. [b] Seetula, J. A.; Feng, Y.; Gutman, D.; Seakins, P. W.; Pilling, M. J. *J. Phys. Chem.* **1991**, *95*, 1658. The 0 K value given above has been converted from a $\Delta_f H_{298}$ value by using a calculated enthalpy change for SiH_3 of $H(298) - H(0) = 0.106$ eV and elemental enthalpy changes from ref 52. The enthalpy change accounts for the translational, rotational, and vibrational heat capacities but not the electronic as the necessary molecular information is not available. Vibrational frequencies are taken from: Ho, P.; Coltrin, M. E.; Binkley, J. S.; Melius, C. F. *J. Phys. Chem.* **1985**, *89*, 4647. [c] Johnson, R. D.; Tsai, B. P.; Hudgens, J. W. *J. Chem. Phys.* **1989**, *91*, 3340. [d] Frey, H. M.; Walsh, R.; Watts, I. M. *J. Chem. Soc., Chem. Commun.* **1986**, 1189. The 0 K value given above has been converted from a $\Delta_f H_{298}$ value by using a calculated enthalpy change for SiH_2 of $H(298) - H(0) = 0.104$ eV, see footnote *b*, and elemental enthalpy changes from ref 52. Vibrational frequencies are taken from: Fredlin, L.; Hauge, R. H.; Kafafi, Z. H.; Margrave, J. L. *J. Chem. Phys.* **1985**, *82*, 3452. [e] Berkowitz, J.; Ruscic, B. In *Vacuum Ultraviolet Photoionization and Photodissociation of Molecules and Clusters*; Ng, C. Y., Ed.; World Scientific: Singapore, 1991; pp 1–41. The 0 K value given above has been converted from a $\Delta_f H_{298}$ value by using an enthalpy change for SiH of $H(298) - H(0) = 0.096$ eV and elemental enthalpy changes from ref 52. [f] Fisher, E. R.; Kickel, B. L.; Armentrout, P. B. *J. Phys. Chem.* **1993**, *97*, 10204. [g] Reference 24.

possibilities. Errors in threshold values, determined by the variation in E_0 among several data sets for all acceptable models and the absolute uncertainty in the energy scale, are believed to be reasonable measures of the absolute accuracy of these threshold values. Errors associated with differences in the energy scale for the different isotopes of silicon are negligible compared to these errors. The general form of eq 1 has been derived as a model for translationally driven reactions[21] and has been found to be quite useful in describing the shapes of endothermic reaction cross sections and in deriving accurate thermochemistry (within the stated error limits) for a wide range of systems.[22]

At elevated energies, some of the observed reaction cross sections begin to decline. This can be because of dissociation of the product ion or competition with other product channels. We have previously discussed a model for product dissociation which makes a simple statistical assumption within the constraints of angular momentum conservation.[23] The model is controlled by two parameters: p, which is an adjustable parameter, and E_D, which is the energy at which product decomposition or competition becomes effective.

Derivation of Bond Energies. The threshold energy, E_0, for a reaction like process 2 is converted to a thermochemical value of interest by using eq 3.

$$M^+ + BC \rightarrow MB^+ + C \quad (2)$$

$$D_0(M^+-B) = \Delta_f H_0(B) + \Delta_f H_0(C) - \Delta_f H_0(BC) - E_0 \quad (3)$$

This expression assumes that there are no activation barriers in excess of the endothermicity of the reaction. This assumption is generally true for gas-phase ion–molecule reactions and has been explicitly tested a number of times.[22] The required literature thermochemistry for the silicon species is listed in Table 2.

Results

Atomic transition metal ions are observed to react with silane according to processes 4–9, where M can refer to Sc, Y, La, and Lu.

$$M^+ + SiH_4 \rightarrow MH^+ + SiH_3 \quad (4)$$
$$\rightarrow MH_2^+ + SiH_2 \quad (5)$$
$$\rightarrow MSi^+ + 2H_2 \quad (6)$$
$$\rightarrow MSiH^+ + H_2 + H \quad (7)$$
$$\rightarrow MSiH_2^+ + H_2 \quad (8)$$
$$\rightarrow MSiH_3^+ + H \quad (9)$$

Another possible reaction channel is formation of $SiH_3^+ + MH$ which is observed in the reaction of silane with all of the other first-row metal ions except titanium.[6–8] Despite a careful search, we did not observe formation of this product for ground or excited electronic states of the group 3 metals. This is easily rationalized if the ionization energies (IEs) of the metal hydrides are all lower than IE(SiH_3), Table 2. This is true for ScH, where IE(ScH) = 6.2 ± 0.2 eV,[24] and seems likely for the other group 3 metal hydrides given the low IEs of the metal atoms.[25,26] The $MSiH_4^+$ adduct also was not observed in any system, establishing that the cross sections for these two products are below 10^{-17} cm^2.

There are two complexities associated with analyzing the cross sections for these systems. First, because silicon exists as the ^{28}Si (92.27% natural abundance), ^{29}Si (4.68% natural abundance), and ^{30}Si (3.05% natural abundance) isotopes, the results obtained for a given m/z ratio can represent several product species. This is straightforward to account for, and the cross sections presented here are total cross sections for all isotopes of a single chemical species.[27] Second, in order to accurately determine absolute magnitudes of product cross sections, ion transmission must be maximized, but this can require mass resolution conditions that do not completely separate signals from adjacent masses. In the present study, cross sections were measured under high resolution conditions (<10% overlap between ions one mass unit apart) to determine the relative intensity of the products and under low mass resolution conditions (sufficiently low that further reductions in resolution do not enhance the product intensity) to verify efficient product collection. Because the kinetic energy dependence of different product ions is very distinct, it is straightforward and unambiguous to correct the cross sections for any deficiencies discovered by this comparison.

Surface Ionization Results. Product cross sections for the reactions of Sc^+, Y^+, La^+, and Lu^+ produced in the SI ion source are shown as a function of translational energy in Figures 1–4. The results for the group 3 ions are quite similar to those seen in the reactions of Ti^+, V^+, and Cr^+ with silane,[6] although MH_2^+ is not observed for Ti^+, V^+, and Cr^+. The dominant processes at low energies are formation of $MSiH_2^+ + H_2$ in

(21) Chesnavich, W. J.; Bowers, M. T. *J. Phys. Chem.* **1989**, *79*, 900.
(22) Armentrout, P. B. In *Advances in Gas Phase Ion Chemistry*; Adams, N. G., Babcock, L. M., Eds.; JAI Press: Greenwich, 1992; Vol. 1, pp 83–119.
(23) Weber, M. E.; Elkind, J. L.; Armentrout, P. B. *J. Chem. Phys.* **1986**, *84*, 1521.
(24) Derived from thermochemistry collected in: Armentrout, P. B.; Sunderlin, L. S. In *Transition Metal Hydrides*; Dedieu, A., Ed.; VCH: New York, 1992; p 1.
(25) Moore, C. E. *Natl. Stand. Ref. Data Ser. (U.S. Natl. Bur. Stand.)* **1971**, *35*.
(26) Martin, W. C.; Zalubas, R.; Hagan, L. *Natl. Stand. Ref. Data Ser. (U.S. Natl. Bur. Stand.)* 1978, *60*.
(27) For example, in the case of $^{45}Sc^+$, the product at m/z 74 can be due to $Sc^{28}SiH^+$ and $Sc^{29}Si^+$. The cross section for $Sc^{29}Si^+$ is calculated by taking the cross section for m/z 73 (due exclusively to $Sc^{28}Si^+$) and scaling it by the ^{28}Si:^{29}Si isotope ratio, 0.051. Subtraction of this cross section from the m/z 74 cross sections yields the cross section due entirely to $Sc^{28}SiH^+$. A similar procedure can then be followed for the m/z 75 (due to $Sc^{28}SiH_2^+$, $Sc^{29}SiH^+$, and $Sc^{30}Si^+$) and m/z 76 (due to $Sc^{28}SiH_3^+$, $Sc^{29}SiH_2^+$, and $Sc^{30}SiH^+$) cross sections. The cross sections for $Sc^{28}SiH_x^+$ product ions are then scaled by 1.084 (accounting for the natural abundance of ^{28}Si) to yield the results presented here for a single chemical species. This same general procedure was used for all three metal systems.

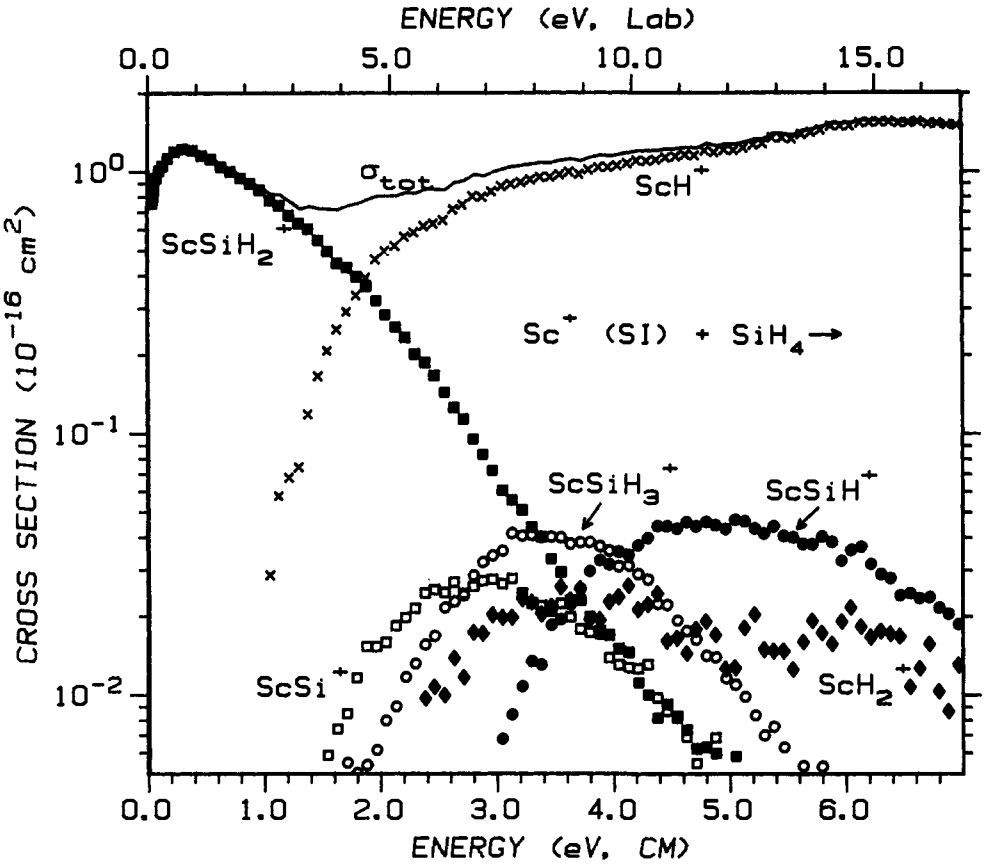

Figure 1. Variation of product cross sections for the reaction of Sc^+ (produced in the surface ionization source) with silane as a function of translational energy in the laboratory frame (upper scale) and the center-of-mass frame (lower scale).

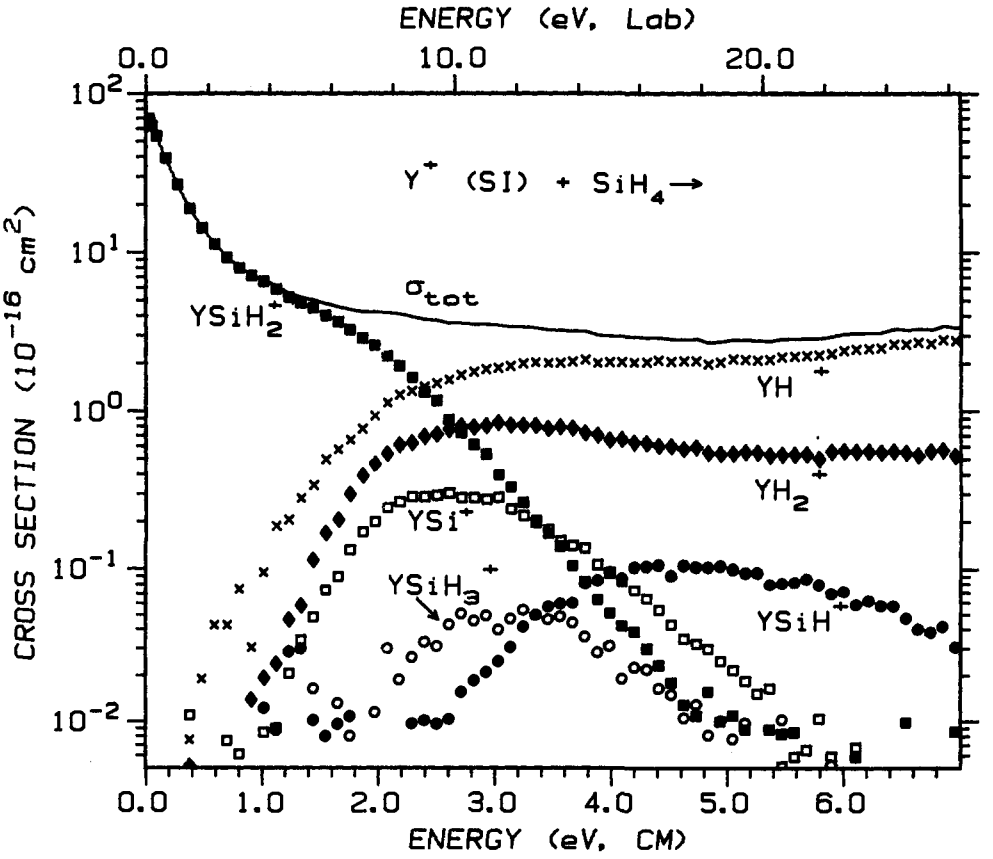

Figure 2. Variation of product cross sections for the reaction of Y^+ (produced in the surface ionization source) with silane as a function of translational energy in the laboratory frame (upper scale) and the center-of-mass frame (lower scale).

reaction 8. As the cross sections for $MSiH_2^+$ decline, the cross sections for formation of MH^+ (M = Sc, Y, La, and Lu) and MH_2^+ (M = Y, La, and Lu) increase concomitantly. The depletion of $MSiH_2^+$ could also be caused by dissociation to

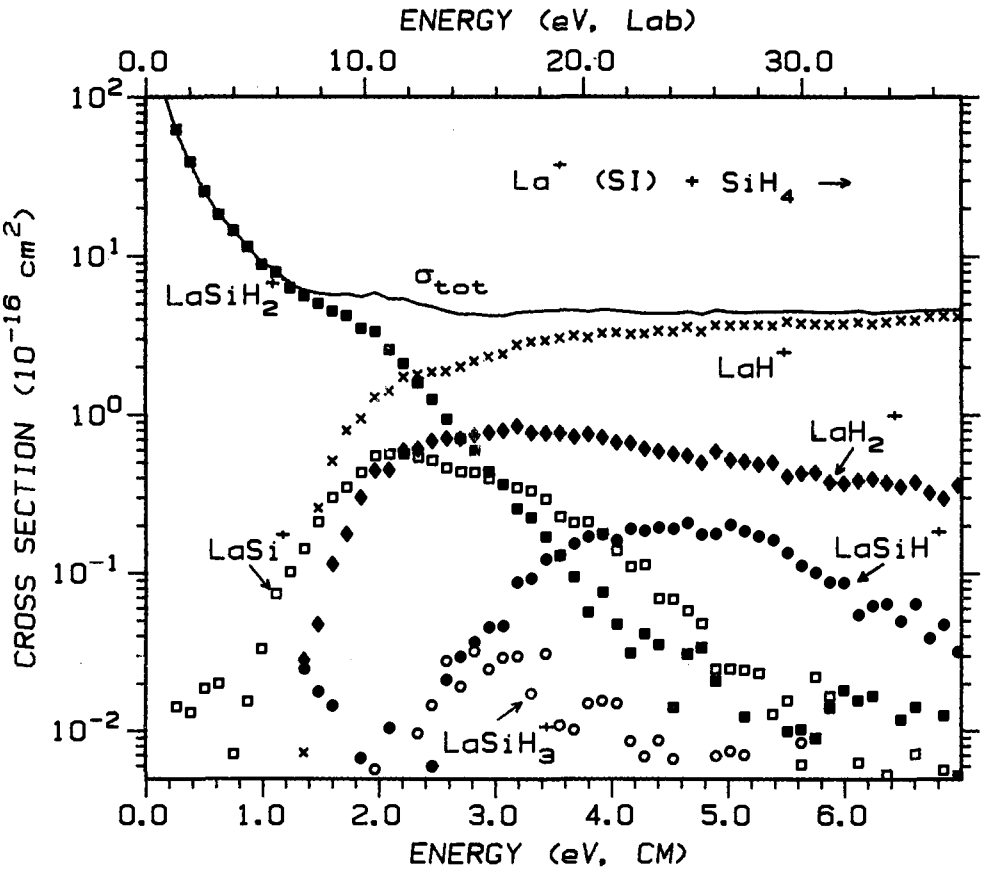

Figure 3. Variation of product cross sections for the reaction of La^+ (produced in the surface ionization source) with silane as a function of translational energy in the laboratory frame (upper scale) and the center-of-mass frame (lower scale).

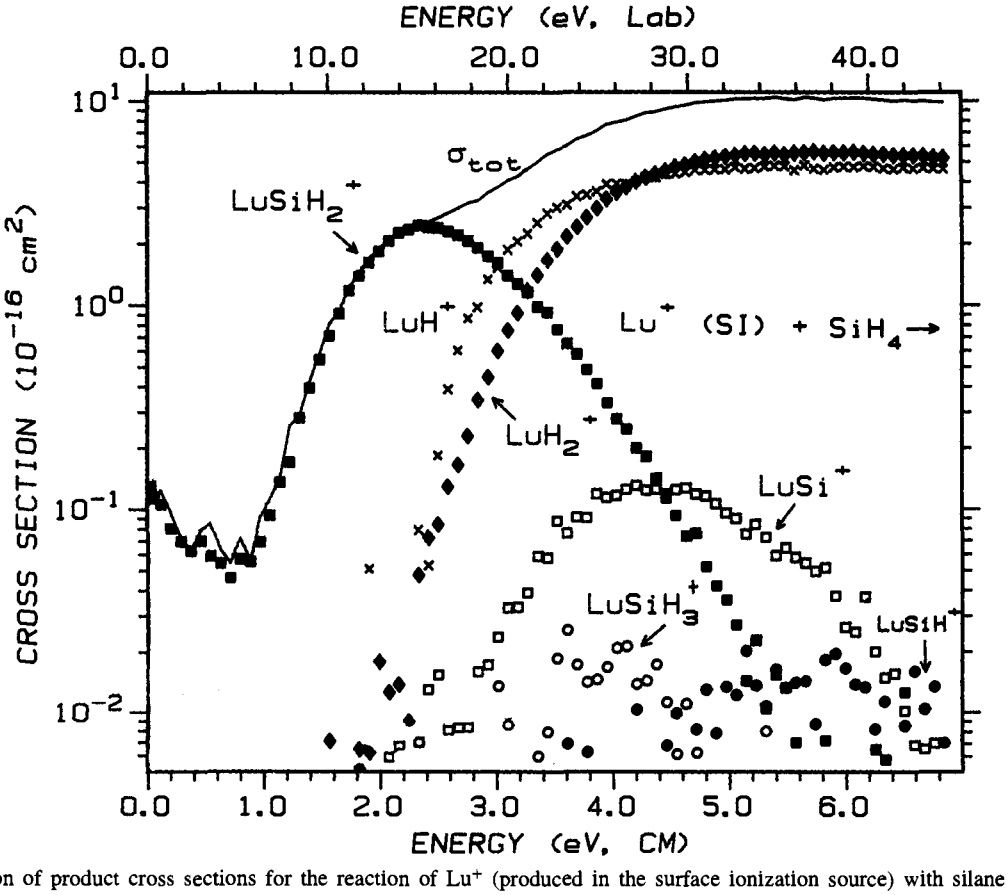

Figure 4. Variation of product cross sections for the reaction of Lu^+ (produced in the surface ionization source) with silane as a function of translational energy in the laboratory frame (upper scale) and the center-of-mass frame (lower scale).

form $M^+ + SiH_2$, which can begin at 2.39 ± 0.07 eV, but the smooth behavior of the sum of the $MSiH^+$, MH^+, and MH_2^+ product cross sections suggests that competition with reactions 4 and 5 is the dominant depletion pathway. The efficiency of

reaction 4 increases from Sc^+ to Y^+ to La^+ to Lu^+. The efficiency of reaction 5 increases from Sc^+ to Y^+ which is comparable to La^+ and then increases for Lu^+, where it is slightly larger than the MH^+ cross section.

At the lowest energies, the $MSiH_2^+$ (M = Y and La) cross sections are large and increase with decreasing energy indicating efficient exothermic reactions. In contrast, the $ScSiH_2^+$ cross section increases with *increasing* energy at the lowest energies, indicating an endothermic reaction that is less efficient by about an order of magnitude above 0.3 eV. The $LuSiH_2^+$ cross section exhibits two features, Figure 4. The low-energy feature is approximately three orders of magnitude smaller than those for M = Y and La and increases with decreasing energy, indicating an exothermic reaction with no barriers in excess of the asymptotic energy of the reactants. The second feature rises from an apparent threshold of ~0.5 eV. It seems likely that these features correspond to reactivity of the a^3D first excited (0.4% of the ion beam at 2250 K) and a^1S (99.6% of ion beam at 2250 K) ground states of Lu^+, respectively, but this conclusion is not definitive.

These results are in reasonable agreement with those of Geribaldi and co-workers.[9] Both studies observe that the reaction of silane with Sc^+ is slow and endothermic and that with Y^+ is rapid and exothermic. Geribaldi and co-workers did not observe reactions of Lu^+ and silane at thermal energies, while we find inefficient reactivity, ≤ 0.1 Å^2. This could be because they have no excited state Lu^+ or because this level of reactivity is below the detection limit of the previous experiment. Geribaldi and co-workers observe that the reaction of silane with translationally excited Sc^+ also forms $SiH_3^+ + ScH$, a product not observed in the present results. Neither do we observe this product for reaction of silane with Ti^+. It is only a small (<0.02 Å^2) product channel for V^+ and Cr^+,[6] where IE(MH) < IE(SiH_3), but it is an important process for the later transition metals where IE(MH) is more similar to IE(SiH_3).[7,8] Based on the similarities of Sc^+ to the early transition metals, we would not expect to observe the hydride abstraction reaction, especially considering that formation of $SiH_3^+ + ScH$ has a calculated threshold energy of 3.4 ± 0.2 eV (Tables 2 and 4), well above that for the $ScH^+ + SiH_3$ which competes directly. The reason why Geribaldi and co-workers observe this process is not immediately clear; however, the possibility exists that formation of SiH_3^+ occurs by reaction of excited states of Sc^+, a reasonable possibility given the laser ablation method used by Geribaldi and co-workers to generate Sc^+.

Reactions 6, 7, and 9 occur at higher energies and are relatively inefficient in all four systems. The decline of the MSi^+ cross sections occurs at about 2.5−3.0 eV. Such a decline could be caused by dissociation to form $M^+ + Si + 2H_2$; however, this process is not possible until 4.20 ± 0.04 eV. Because MSi^+ must be formed by dehydrogenation of the $MSiH_2^+$ product, the decline in the MSi^+ cross sections must be due to depletion of the intermediate that is the precursor to $MSiH_2^+$ formation. The smooth appearance of the sum of the cross sections for $MSiH^+$ and $MSiH_3^+$ products, particularly for M = Sc and Y, suggests that these two products are closely coupled. Therefore, we believe that the $MSiH_3^+$ cross sections decline at higher energies because the product dehydrogenates to form $MSiH^+ + H_2$. This is consistent with the results of the reactions of silane with Ti^+, V^+, and Cr^+,[6] and Fe^+, Co^+, and Ni^+.[7]

Flow Tube Results. Comparison of the product cross sections for La^+ and Lu^+ produced in the SI and DC/FT ion sources reveals that, within experimental error, the cross section magnitudes and energy dependences are the same for the two sources. Therefore the DC/FT data for La^+ and Lu^+ are not shown. This result and its implications are discussed further below. The equivalency of the SI and DC/FT data is expected for Lu^+ because no large changes in electronic state population occur (Table 1), although we might have expected that the low-energy feature in the $LuSiH_2^+$ cross section would decrease if the excited states are being quenched in the flow tube. However, quenching could be inefficient in this case because the ground and excited states of Lu^+ are widely separated (unlike the other three systems), making collisional quenching inefficient.[28] The constancy of the magnitude of this feature indicates that either the excited state populations are serendipitously the same for ions produced in the SI and DC/FT sources or the low-energy feature is actually due to reaction of the Lu^+ (a^1S) ground state. The latter possibility would mean that there are two distinct mechanisms for this reaction channel, which seems unlikely as there are no indications of this in any of the other metal systems studied here or previously.[6-8] However, this latter possibility would mean that the Lu^+-SiH_2 bond energy exceeds 2.39 eV.

Product cross sections for the reactions of Sc^+ and Y^+ produced in the DC/FT ion source are shown as a function of translational energy in Figures 5 and 6. Comparison of Figures 1 and 2 to Figures 5 and 6 shows that the cross section magnitudes and product distributions for Sc^+ and Y^+-formed in the SI and DC/FT ion sources are markedly different. This comparison shows that the reactivity of Sc^+ (SI) is greater than that observed for Sc^+ (DC/FT). The same product channels are observed for both sources with the exception of formation of $ScH_2^+ + SiH_2$, reaction 5, which is observed only for reaction of silane with Sc^+ generated in the SI source. The threshold energies for the Sc^+ (SI) results are shifted to lower energies by 0.2 to 0.4 eV compared to the Sc^+ (DC/FT) results. The difference in product distribution and the shift in threshold energies found in the SI data are consistent with contributions to the reactivity from the a^1D first excited state of Sc^+.

Comparison of Figures 2 and 6 shows that the overall reactivity of Y^+ (SI) is less than that observed for Y^+ (DC/FT), the opposite result as that for Sc^+. The same products are observed for Y^+ ions created in both sources. Careful examination of the threshold energies for the SI and DC/FT results shows that the Y^+ (DC/FT) thresholds are shifted to higher energies by 0.1−0.2 eV, consistent with contributions to the reactivity from the a^3D first excited state of Y^+.

By using a procedure analogous to one outlined previously for Co^+,[29] we use eq 1 to analyze the energy-dependent cross sections for ions generated in the DC/FT and SI sources in a self-consistent fashion. Given the known temperature for the SI source, the results suggest that the populations of the electronic states of Sc^+ generated in the DC/FT source can be characterized by a Maxwell−Boltzmann distribution at 400 ± 200 K. The results for Y^+, La^+, and Lu^+ are not as clear because the thresholds for various endothermic processes are sufficiently high that changes in thresholds which occur when the effective temperature of the DC/FT generated ions is changed are not large enough to allow us to accurately determine the characteristic temperature. Other studies in our laboratory that compare the reactivity of H_2, HD, and D_2 with Y^+ generated by the SI and DC/FT sources indicate that the electronic temperature of the Y^+ is 300 ± 100 K.[30] Because we are unable to directly determine the characteristic temperature of the DC/

(28) Loh, S. K.; Fisher, E. R.; Lian, L.; Schultz, R. H.; Armentrout, P. B. *J. Phys. Chem.* **1989**, *93*, 3159.
(29) Haynes, C. L.; Armentrout, P. B. *Organometallics* **1994**, *13*, 3480.
(30) Chen, Y.-M.; Armentrout, P. B. *J. Phys. Chem.*, manuscript in preparation.

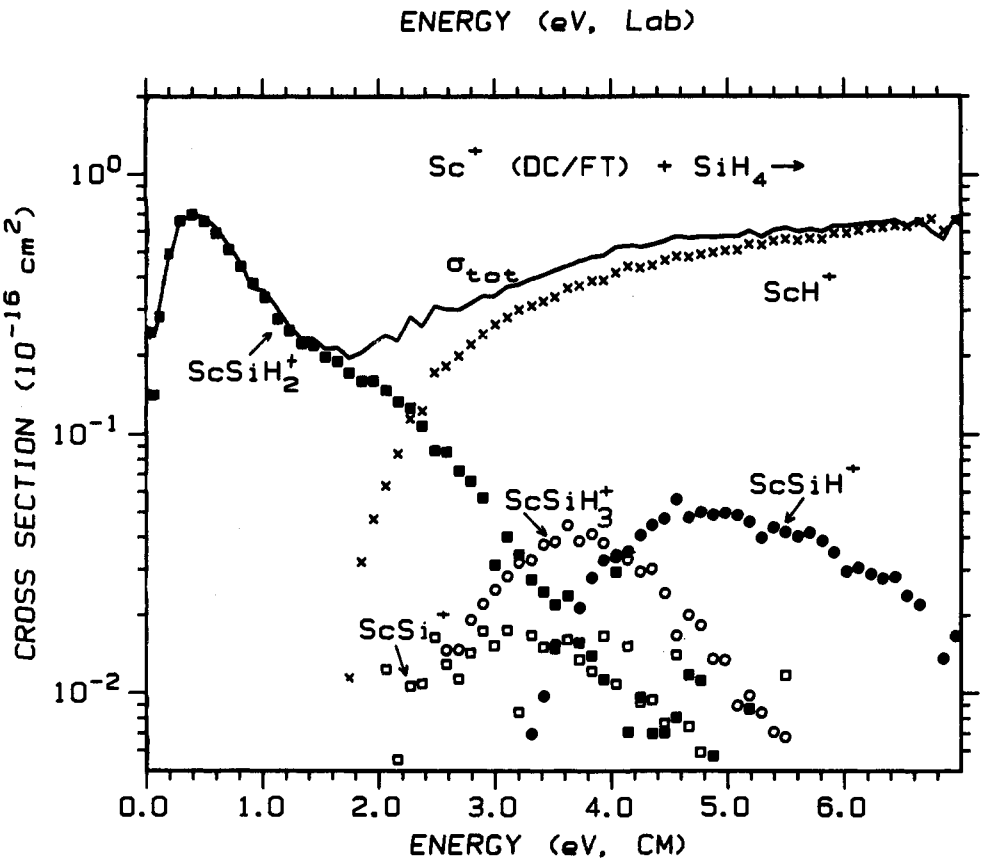

Figure 5. Variation of product cross sections for the reaction of Sc^+ (a^3D, produced in the flow tube/dc-discharge source) with silane as a function of translational energy in the laboratory frame (upper scale) and center-of-mass frame (lower scale).

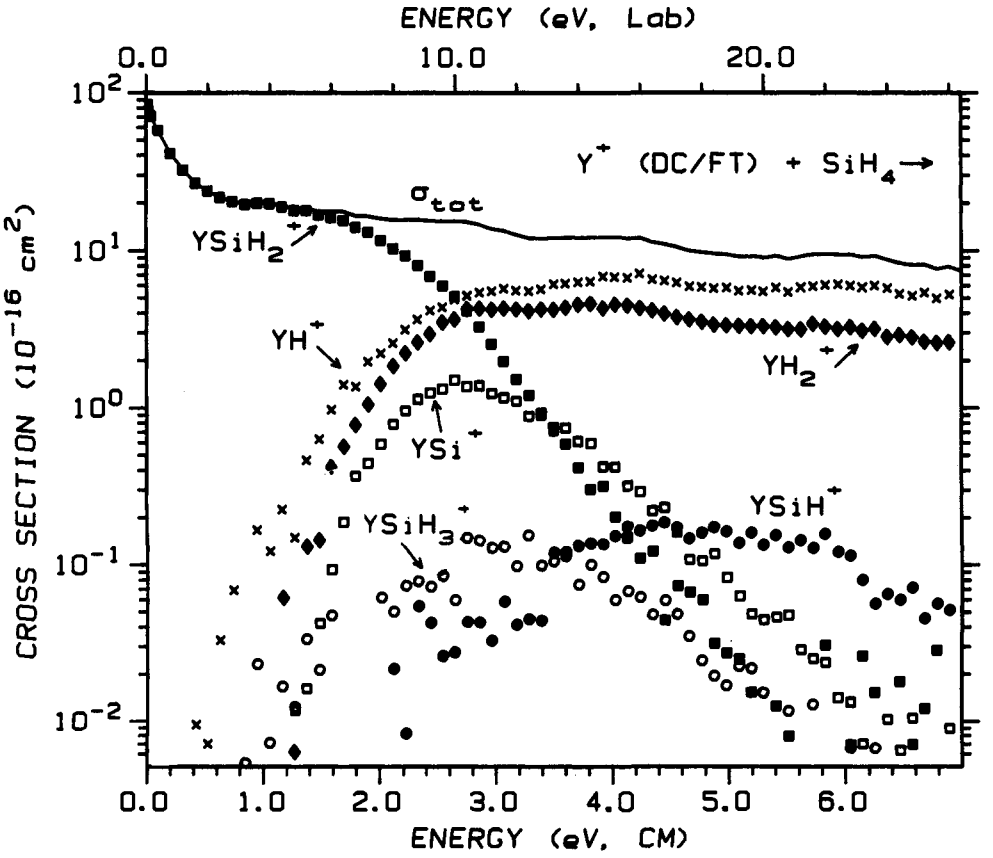

Figure 6. Variation of product cross sections for the reaction of Y^+ (produced in the flow tube/dc-discharge source) with silane as a function of translational energy in the laboratory frame (upper scale) and center-of-mass frame (lower scale).

FT generated La^+ and Lu^+ ions we assume that the state distribution of these metals can be characterized by an effective temperature of ≤2250 K, as suggested by the very similar results for reaction of the Lu^+ and La^+ ions generated in the SI and

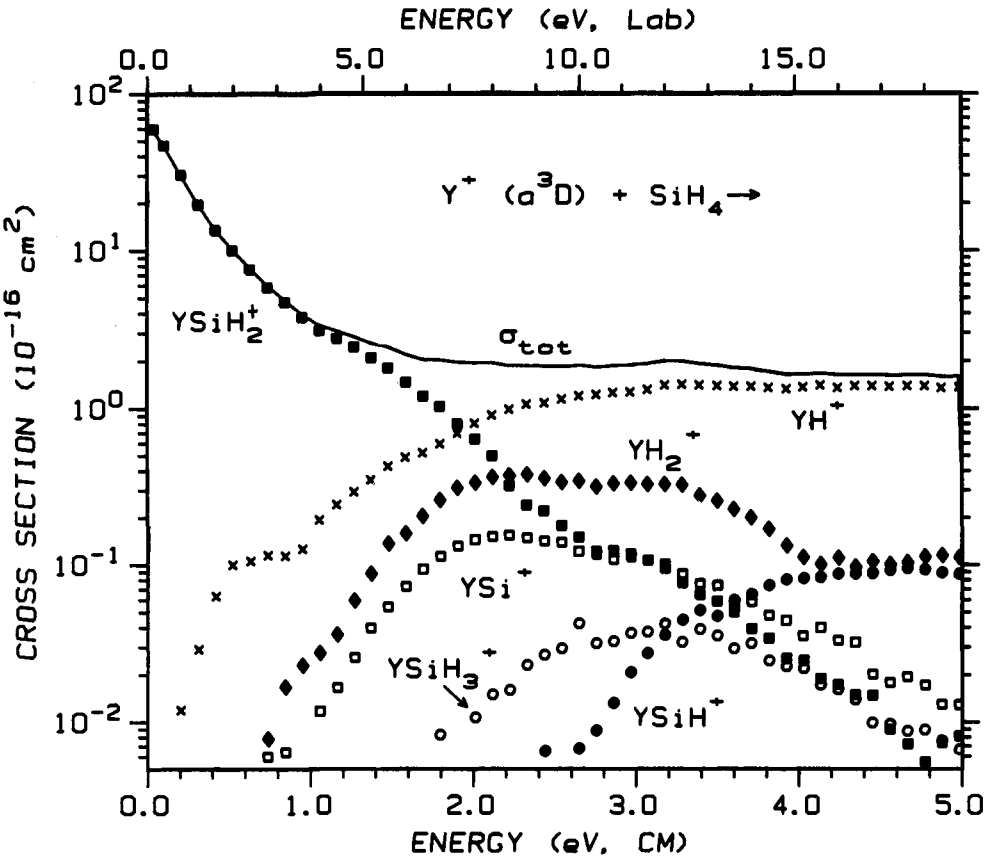

Figure 7. Variation of product cross sections for the reaction of Y^+ (a^3D) with silane as a function of translational energy in the laboratory frame (upper scale) and center-of-mass frame (lower scale). The cross sections shown correspond to results for Y^+ largely in the a^3D state (91%), with small contributions from the second and third excited states, a^1D (7.9%) and a^3F (1.3%), respectively, see text.

DC/FT sources. It is possible that the actual electronic temperature of the DC/FT beams could be considerably lower, in analogy with the DC/FT results for Sc^+ and Y^+. It was verified that the uncertainty in this temperature has no influence on the thermochemical results for La^+ and Lu^+ (assuming that all states are equally reactive, the only sensible assumption in the absence of definitive information to the contrary). The populations of the electronic states of the ions at both temperatures are listed in Table 1.

State-Specific Reactivity. To explicitly examine the relative contributions of the ground and excited electronic states of Sc^+ and Y^+, we extract state-specific cross sections for reaction of these ions with silane. The conversion of the raw SI and DC/FT data to state-specific data is relatively straightforward. For yttrium, the SI ion beam at 2250 ± 100 K consists of 11.4% Y^+ (a^1S), 80.6% Y^+ (a^3D), 6.9% Y^+ (a^1D), and 1.1% Y^+ (a^3F). To extrapolate to the state-specific behavior of Y^+ excited electronic states, the DC/FT data (assumed to be 91.5% a^1S and 8.5% a^3D) are scaled by a factor of 0.125 (0.114/0.915) and subtracted from the SI data. The remaining cross section is divided by 0.875 to readjust to 100%. The resulting cross section, shown in Figure 7, largely comprises a^3D (91%), with small contributions from the second and third excited states, a^1D (7.9%) and a^3F (1.3%), respectively. We then use the state-specific a^3D cross section to correct the DC/FT data for the 8.5% contribution from this excited state in a similar manner. The results for Y^+ (a^1S) are shown in Figure 8. Iterating this procedure one more time does not lead to any changes in the derived state-specific cross sections. The details of this process assume that the Y^+ (DC/FT) beam can be characterized by an electronic temperature of 300 ± 100 K.[30] If we assume that the Y^+ beam may be characterized by the upper limit of 400 K, the Y^+ (a^1S) cross sections derived have the same shape as those shown in Figure 8, but are a factor of ~1.2 larger. The Y^+ (a^3D) cross sections derived assuming the two different temperatures have the same shape and magnitude.

The extraction of Sc^+ (a^1D) excited state cross sections is completed in a procedure analogous to that described above; however, because we assume the FT/DC data are 100% Sc^+ (a^3D) ground state, no correction is necessary to obtain ground state data. After removing the Sc^+ (a^3D) ground state cross section from the SI data, we are left with a cross section representing excited state reactivity that is 52.1% a^1D and 47.9% a^3F, Figure 9. Because the contribution of these states is nearly the same, we are unable to directly determine their individual contributions to the excited state reactivity; however, the shift in threshold energies of 0.2−0.4 eV, discussed above, is consistent with the excited state reactivity being largely due to the a^1D state (Table 1). For brevity, in the remainder of the discussion, the excited state behavior of Y^+ and Sc^+ shown in Figures 7 and 9 is referred to as Y^+ (a^3D) and Sc^+ (a^1D, a^3F), respectively.

Comparison of the state-specific data for Sc^+ shows that the ground state a^3D exhibits a different product distribution and is less reactive than the a^1D and a^3F excited states. Formation of $ScSiH_2^+ + H_2$, reaction 4, is exothermic for Sc^+ (a^1D, a^3F) and an order of magnitude larger than that for the Sc^+ (a^3D) state, consistent with the 0.315 and 0.608 eV excitation energies of the a^1D and a^3F states, respectively. The cross section for reaction 4 increases by more than an order of magnitude for the a^1D, a^3F states while that for $ScSi^+$ is a factor of 5 larger than the a^3D state. The $ScSiH^+$ and $ScSiH_3^+$ cross sections show no enhancement for excited vs ground state Sc^+. Figure 9 does not show cross sections for $ScSiH^+$ and $ScSiH_3^+$ because

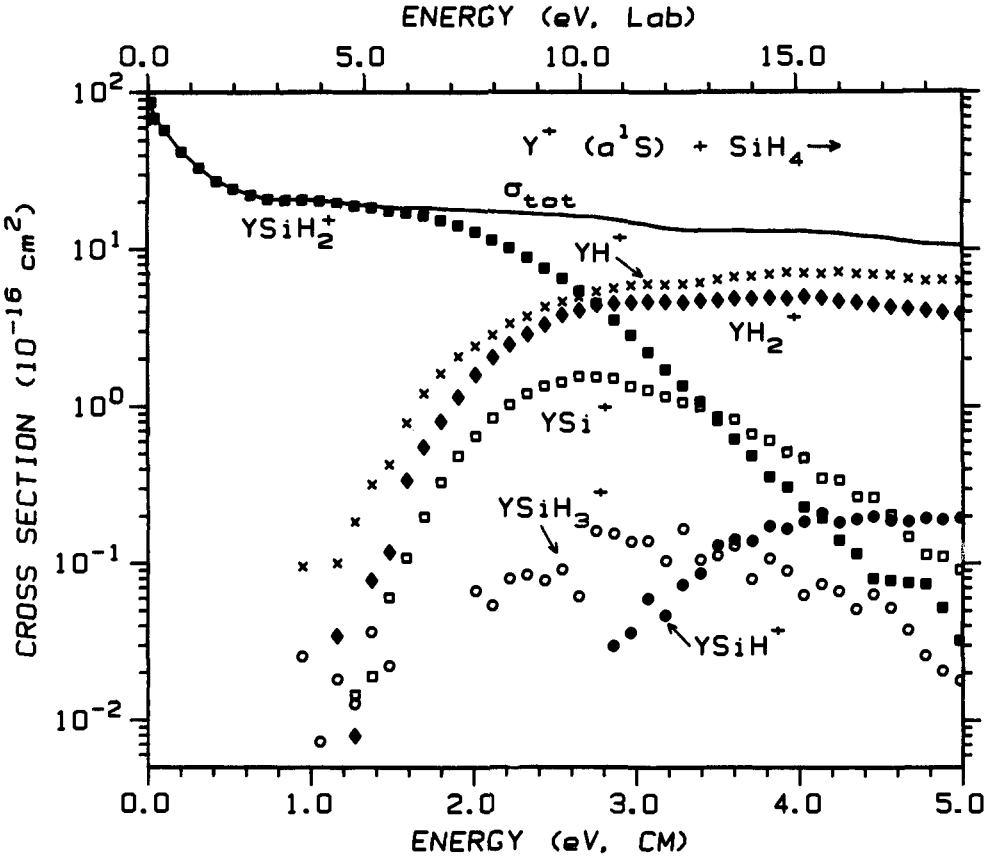

Figure 8. Variation of product cross sections for the reaction of Y^+ (a^1S) with silane as a function of translational energy in the laboratory frame (upper scale) and center-of-mass frame (lower scale).

the SI and DC/FT results for these products are very similar, making extraction of the excited state reaction cross sections unreliable.

Comparison of the state-specific data for Y^+ shows that the a^1S ground state is more reactive than the a^3D excited state. For the $YSiH_2^+$ cross sections at energies below 1.2 eV (where competition with other channels begins to affect these cross sections), the a^1S and a^3D cross sections decline as $E^{-0.5\pm0.1}$ and $E^{-1.4\pm0.2}$, respectively. This difference is discussed further below. The cross sections for reactions 5 and 6 increase by an order of magnitude, those for reactions 4 and 9 increase by a factor of 4, and that for reaction 7 increases by a factor of 2 for the a^1S ground state compared to the a^3D excited state.

Thermochemistry. The threshold regions of the cross sections for SI and DC/FT data are analyzed by using eq 1. The analyses of the DC/FT data (Sc^+, Y^+, La^+, and Lu^+) as well as the SI data for La^+ and Lu^+ are summarized in Table 3, and in all cases, the model of eq 1 accurately reproduces the experimental results. The SI results for Sc^+ and Y^+ are complicated due to the drastically different reactivities of the ground and excited states of these ions, as discussed above. For $M^+ = Y^+$, La^+, and Lu^+ formed in the DC/FT source and Lu^+ (SI), the cross sections for $MSiH^+$ and $MSiH_3^+$ are small enough that we are unable to definitively model the results. Results for the analyses of state-specific cross section information for Sc^+ and Y^+ are also listed in Table 3.

Average threshold energies (all E_0 values available in Table 3; DC/FT and state-specific a^1D, a^3F results for Sc^+; DC/FT, state-specific a^1S, and state-specific a^3D results for Y^+; and DC/FT and SI results for La^+ and Lu^+) are combined with literature thermochemistry in eq 3 to determine 0 K bond energies for M^+-SiH_x ($x = 0-3$) for M = Sc, Y, La, and Lu. These bond energies, which have not been determined previously, are listed in Table 4.

MH^+ and MH_2^+ Bond Energies. The literature BDEs for MH^+ for M = Sc, Y, La, and Lu listed in Table 4 are obtained from the reactions of H_2 and D_2 with metal ions produced by surface ionization.[31] The thresholds for reactions 4 (Table 3) lead to $D_0(M^+ - H)$ values of 2.27 ± 0.11, 2.44 ± 0.13, 2.36 ± 0.05, and 1.81 ± 0.24 eV, respectively. These values are somewhat lower than the respective literature BDEs, Table 4, although within the combined experimental uncertainties. There are two possible explanations for this systematic difference. First, the thresholds for reactions 4 are elevated because of competition with the dehydrogenation reaction 8. Second, because the thresholds measured here correspond to reactions of silane with metal ions in their ground states, they are not subject to complications from reactivity of low-lying excited states. Such complications could have yielded elevated BDEs in the previous study.[31] Indeed, we have recently reexamined the reactions of H_2, HD, and D_2 with Y^+ produced in the DC/FT source and determined $D_0(Y^+-H) = 2.59 \pm 0.06$ eV, within experimental error of the value measured here. Additional studies of these possibilities are warranted in the other metal systems as well.

The threshold measured for ScH_2^+ formation from Sc^+ (a^1D, a^3F) is 1.84 ± 0.17 eV. This can be compared to the thermodynamic thresholds calculated from Tables 2 and 4 for reaction of the a^1D state, 1.72 ± 0.10 eV, and the a^3F state, 1.43 ± 0.10 eV. This comparison suggests that formation of $ScH_2^+ + SiH_2$, reaction 5, is produced exclusively by the a^1D state and helps confirm that the extracted Sc^+ (a^1D, a^3F) cross sections are reasonable and that they may be dominated by the a^1D state. The threshold for reaction 5 with Sc^+ (a^1D) yields $D_0(Sc^+-2H) = 4.72 \pm 0.19$ eV, in good agreement with a recent determination of Bushnell et al., 4.715 ± 0.008

(31) Elkind, J. L.; Sunderlin, L. S.; Armentrout, P. B. *J. Phys. Chem.* **1989**, *93*, 3151.

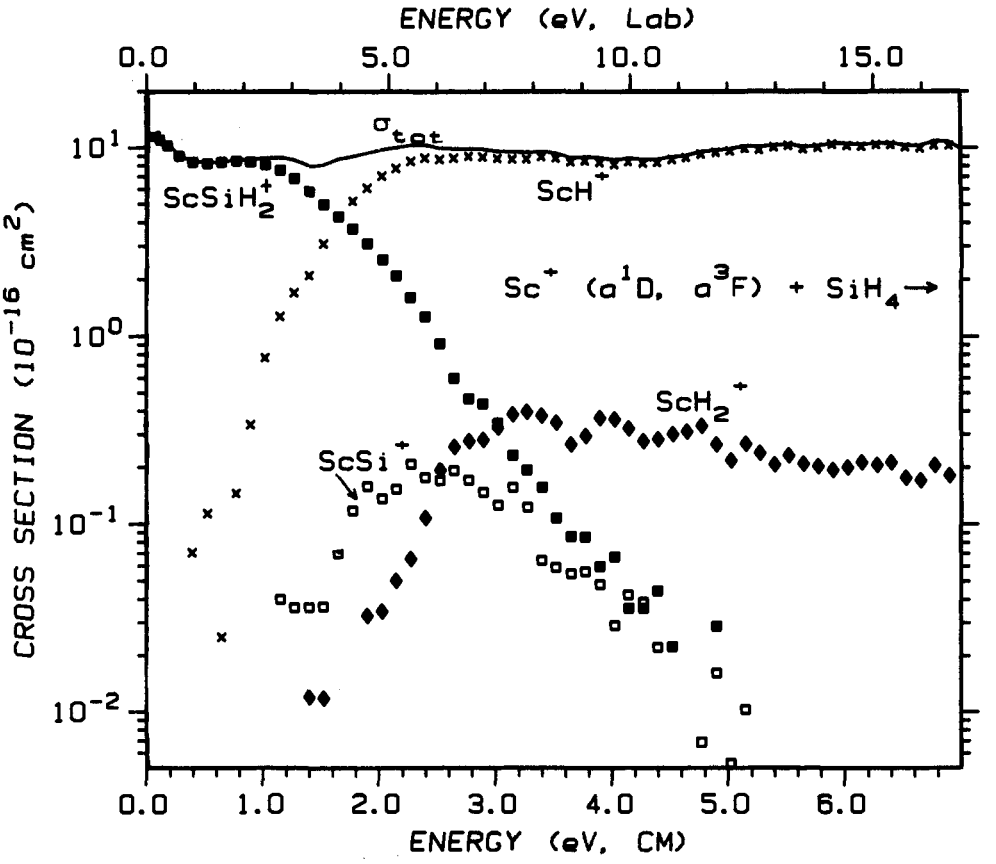

Figure 9. Variation of product cross sections for the reaction of Sc^+ (52.1% a^1D and 47.9% a^3F) as a function of translational energy in the laboratory frame (upper scale) and center-of-mass frame (lower scale). The a^1D state is thought to be largely responsible for the observed reactivity, see text.

eV.[32] It is also in agreement with $D_0(Sc^+-2H) = 4.84 \pm 0.05$ eV,[34] the weighted average of results from our laboratory on the reactions of ethane, propane, and cyclopentane.[33] The $D_0(M^+-2H)$ values determined in the present study for M = Y, La, and Lu are consistent with but somewhat lower than those determined in previous work (Table 4), as evaluated from reactions of ethane with metal ions produced by SI.[34] As noted above for reaction 4, the present values could be low because of competition or could be more accurate because of the availability of state-specific results. Because the result for $D_0(Sc^+-2H)$ obtained here appears to be reliable, we average the present values with the previous ones to obtain $D_0(Sc^+-2H) = 4.82 \pm 0.12$ eV, $D_0(Y^+-2H) = 5.27 \pm 0.11$ eV, $D_0(La^+-2H) = 5.09 \pm 0.08$ eV, and $D_0(Lu^+-2H) = 4.00 \pm 0.16$ eV, which we take as our best values for these bond energies.

Discussion

Comparison of M^+-CH_x and M^+-SiH_x Bond Energies. Table 4 lists the M^+-SiH_x bond dissociation energies (BDEs) measured here along with the available M^+-CH_x BDEs. The metal–silicon BDEs are weaker than the metal–carbon BDEs, and both the metal–carbon and metal–silicon BDEs decrease with increasing number of hydrogen atoms. This is consistent with our previous results for the other first-row transition metal ions (Ti^+ to Zn^+).[6-8] This is also consistent with the theoretical calculations of Cundari and Gordon[10] (based on calculated force constants) and Musaev et al.,[11] who find that the $MSiH_2^+$ complexes have significantly weaker bonds than their MCH_2^+ counterparts.

The bond energies $D(M^+-H)$, $D(M^+-SiH_3)$, $D(M^+-SiH_2)$, $D(M^+ - Si)$ have similar patterns for the group 3 metals: 1.0:0.7:0.9:1.0:1.0 for M = Sc; 1.0:0.8:≥0.9:1.1:1.0 for M = Y; 1.0:0.8≥1.0:1.1:1.2 for M = La. The relationships for M = Lu are not included because of our inability to determine the Lu^+-SiH and Lu^+-SiH_3 bond energies. The M^+-SiH_x (x = 1–3) BDEs, Table 4, tend to increase as we move down the column from scandium to yttrium and lanthanum. This trend is consistent with calculations by Musaev et al. on M^+-SiH_2 for M = Co, Rh, and Ir[11] and with the results of Goddard and co-workers on M^+-H BDEs for M = Sc, Y, and La.[35] The Lu^+-Si and Lu^+-SiH_2 bonds are considerably weaker than those for the other group 3 metals. A similar result is found for the $LuCH_x^+$ (x = 2, 3) bond energies as compared to the other group 3 metal–carbon BDEs. The relative weakness of these BDEs is a consequence of the inert $6s^2$ ground state configuration of Lu^+ and the large promotion energies to open shell configurations that are more suitable for bonding.

Previously, we have discussed the trends of metal–silicon BDEs in terms of comparison to metal–carbon and silicon–silicon BDEs.[6-8] A complete comparison between the metal–carbon and metal–silicon results is not possible because the MCH^+ and MC^+ BDEs are not known. However, a direct comparison of MXH_3^+ vs MXH_2^+ (X = Si, or C) shows a strong increase in BDEs for MCH_3^+ to MCH_2^+, whereas the $MSiH_2^+$ BDEs are only slightly larger than those for $MSiH_3^+$. This suggests that the mode of bonding in the metal–silicon species is not directly analogous to the metal–carbon analogues.

(32) Bushnell, J. E.; Kemper, P. R.; Maitre, P.; Bowers, M. T. *J. Am. Chem. Soc.* **1994**, *116*, 9710.

(33) Sunderlin, L. S.; Aristov, N.; Armentrout, P. B. *J. Am. Chem. Soc.* **1987**, *109*, 78.

(34) Armentrout, P. B.; Kickel, B. L. *Organometallic Ion Chemistry*; Freiser, B. S., Ed.; Kluwer: Dordrecht, 1995; in press.

(35) Ohanessian, G.; Goddard, W. A. *Acc. Chem. Res.* **1990**, *23*, 386. Schilling, J. B.; Goddard, W. A.; Beauchamp, J. L. *J. Phys. Chem.* **1987**, *91*, 5616; *J. Am. Chem. Soc.* **1987**, *109*, 5565.

Table 3. Summary of Optimum Parameters in Eq 1[a]

reaction	E_0, eV	n	σ_0	p	E_D, eV
$Sc^+(DC/FT)^b + SiH_4 \rightarrow$					
$ScH^+ + SiH_3$	1.75(0.06)	1.3(0.1)	0.54(0.06)		
$ScSi^+ + 2H_2$	1.74(0.14)	1.4(0.4)*	0.04(0.01)	2, 3	3.3(0.2)
$ScSiH^+ + H_2 + H$	3.37(0.10)	1.0(0.3)*	0.20(0.03)	1, 2	4.9(0.2)
$ScSiH_2^+ + H_2$	0.22(0.02)	0.3(0.1)	0.46(0.06)	0	0.8(0.1)
$ScSiH_3^+ + H$	2.16(0.16)	1.5(0.5)*	0.09(0.02)	2, 3, 4	3.8(0.2)
Sc^+ (a^1D, a^3F)[c] $+ SiH_4 \rightarrow$					
$ScH^+ + SiH_3$	1.54(0.06)	1.0(0.2)*	15.0(3.3)		
$ScH_2^+ + SiH_2$	2.15 (0.17)	1.5(0.5)*	0.75(0.21)		
$ScSi^+ + 2H_2$	1.64(0.09)	1.4(0.4)*	0.51(0.09)	2, 3	2.8(0.1)
$ScSiH_2^+ + H_2$	<0.00[d]	0.4(0.1)	8.60(2.60)		
$Y^+(DC/FT)^b + SiH_4 \rightarrow$					
$YH^+ + SiH_3$	1.44(0.18)	1.6(0.6)*	8.99(2.60)		
$YH_2^+ + SiH_2$	1.74(0.07)	1.3(0.3)	10.1(0.30)		
$YSi^+ + 2H_2$	1.78(0.12)	1.4(0.7)*	5.03(0.65)	2, 3	2.7(0.2)
$YSiH^+ + H_2 + H$	2.92(0.19)	1.4(0.7)*	0.60(0.18)	1, 2	4.7(0.3)
$YSiH_2^+ + H_2$	<0.00[d]	0.6(0.1)	18.1(0.36)		
$Y^+(a^1S)^e + SiH_4 \rightarrow$					
$YH^+ + SiH_3$	1.51(0.14)	1.4(0.3)	9.85(2.16)		
$YH_2^+ + SiH_2$	1.78(0.12)	1.1(0.3)	11.7(1.62)		
$YSi^+ + 2H_2$	1.74(0.10)	1.4(0.4)*	5.29(0.75)	2, 3	2.7(0.2)
$YSiH^+ + H_2 + H$	2.88(0.24)	1.4(0.7)*	0.56(0.19)	1, 2	4.5(0.2)
$YSiH_2^+ + H_2$	<0.00[d]	0.5(0.1)	18.2(0.88)		
$Y^+(a^3D)^f + SiH_4 \rightarrow$					
$YH_2^+ + SiH_2$	1.48(0.11)	1.1(0.4)*	1.04(0.11)		
$YSi^+ + 2H_2$	1.53(0.10)	1.1(0.4)*	0.50(0.10)	2, 3	2.6(0.2)
$YSiH^+ + H_2 + H$	2.87(0.14)	1.3(0.3)*	0.26(0.06)	2	4.8(0.2)
$YSiH_2^+ + H_2$	<0.00[d]	1.4(0.2)	4.73(1.76)		
$YSiH_3^+ + H$	1.79(0.16)	1.5(0.5)*	0.10(0.03)	2, 3, 4	3.3(0.2)
$La^+(SI)^g + SiH_4 \rightarrow$					
$LaH^+ + SiH_3$	1.54(0.05)	1.1(0.1)	4.85(0.28)		
$LaH_2^+ + SiH_2$	1.84(0.08)	1.1(0.3)*	2.07(0.27)		
$LaSi^+ + 2H_2$	1.34(0.10)	1.5(0.5)*	1.00(0.14)	2, 3	2.5(0.1)
$LaSiH^+ + H_2 + H$	2.94(0.25)	1.4(0.7)*	0.49(0.18)	1, 2	4.6(0.2)
$LaSiH_3^+ + H$	1.92(0.28)	1.4(0.7)*	0.07(0.04)	2, 3, 4	3.2(0.4)
$La^+(DC/FT)^b + SiH_4 \rightarrow$					
$LaH^+ + SiH_3$	1.57(0.04)	1.2(0.1)	6.02(1.20)		
$LaH_2^+ + SiH_2$	1.76(0.07)	1.0(0.2)*	2.17(0.23)		
$LaSi^+ + 2H_2$	1.32(0.12)	1.4(0.7)*	0.82(0.15)	2, 3	2.5(0.1)
$Lu^+(SI)^g + SiH_4 \rightarrow$					
$LuH^+ + SiH_3$	2.27(0.19)	2.0(0.5)*	5.92(2.25)		
$LuH_2^+ + SiH_2$	3.00(0.09)	1.3(0.3)*	13.1(2.7)		
$LuSi^+ + 2H_2$	3.14(0.14)	1.4(0.7)*	0.58(0.11)	2, 3	4.4(0.2)
$LuSiH_2^+ + H_2$	1.40(0.09)	1.5(0.5)*	6.40(0.74)	3	2.5(0.1)
$Lu^+(DC/FT)^b + SiH_4 \rightarrow$					
$LuH^+ + SiH_3$	1.94(0.28)	2.0(0.5)*	4.75(2.49)		
$LuH_2^+ + SiH_2$	2.91(0.18)	1.4(0.4)*	11.2(3.46)		
$LuSi^+ + 2H_2$	3.04(0.19)	1.4(0.7)*	0.46(0.11)	2	4.4(0.2)
$LuSiH_2^+ + H_2$	1.42(0.09)	1.5(0.5)*	7.27(0.90)	3	2.5(0.1)

[a] Uncertainties are in parentheses. Asterisks represent those analyses where the value of n is fixed over the indicated range, see text. [b] Ions generated in the dc-discharge/flow tube (DC/FT) source. This source produces predominantly ground state Sc^+, Y^+, La^+, and Lu^+ ions. Cross sections are analyzed without a distribution of electronic states. Once the threshold has been determined with the model of eq 1, the average electronic energy of M^+ at 400 K for Sc^+ (0.011 eV) and 300 K for Y^+ (0.010 eV), La^+ (0.002 eV), and Lu^+ (0.000 eV) is included to give E_0, see text. [c] Sc^+ (a^1D, a^3F) state-specific cross sections are analyzed without a distribution of electronic states. Once the threshold has been determined with the model of eq 1, the average electronic energy of Sc^+ (a^1D) at 2250 K (0.315 eV) is included to give E_0, the threshold for reaction of Sc^+ (a^3D_1) at 0 K. [d] Exothermic reaction. [e] State-specific cross sections for ground state Y^+ (a^1S). [f] Y^+ (a^3D) state-specific cross sections are analyzed without a distribution of electronic states. Once the threshold has been determined with the model of eq 1, the average electronic energy of Y^+ at 2300 K (0.143 eV) is included to give E_0, the threshold for reaction of Y^+ (a^1S) at 0 K. [g] Ions generated in the surface ionization (SI) source.

We can gain further insight into metal−silicon interactions by comparing to the silicon−silicon bonded analogues. The BDEs $D(H-SiH_3)$, $D(SiH_3-SiH_3)$,[36] $D(H_2Si-SiH_2)$,[37] $D(HSi-SiH)$,[38] and $D(Si-Si)$[39] are related as 1.0:0.8:0.8:1.0:0.8. These silicon−silicon bond energy relationships must be covalent interactions and illustrate the difficulty silicon has in forming multiple bonds. Comparison of these silicon−silicon bond energy relationships to those of the metal−silicon relationships shows a reasonably parallel sequence. Because the silicon−silicon interactions are covalent, the similarity in the bond energy relationships may indicate that the bonding interactions between the group 3 metal ions and silicon ligands are largely covalent. This idea is explored further in the theoretical calculations of Cundari and Gordon,[10] who conclude that the Sc^+-SiH_2 bond is largely (45%) described as a covalent double bond with appreciable (32%) ylide-like ($M^{2+}-SiH_2^-$, corresponding to a high-energy asymptote) contributions where there is both a dative σ bond and a covalent π bond.

(36) $\Delta_f H_0(Si_2H_6)$ = 1 eV taken from: Lias, S. G.; Bartmess, J. E.; Liebman, J. F.; Holmes, J. L.; Levin, R. D.; Mallar, W. G. *J. Phys. Chem. Ref. Data* **1988**, *17*, No. 1.

(37) Kutzelnigg, W. *Angew. Chem., Int. Ed. Engl.* **1984**, *89*, 272.

(38) Ruscic, B.; Berkowitz, J. *J. Chem. Phys.* **1991**, *95*, 2416.

(39) Huber, K. P.; Herzberg, G. *Molecular Spectra and Molecular Structure Constants of Diatomic Molecules*; Van Nostrand Reinhold Company: New York, 1979; and references therein.

Table 4. Experimental Bond Energies at 0 K, eV[a]

L	$D(Sc^+-L)$	$D(Y^+-L)$	$D(La^+-L)$	$D(Lu^+-L)$
H	2.44(0.09)[b]	2.66(0.06)[b]	2.48(0.09)[b]	2.11(0.16)[b]
2H	4.84(0.05)[c]	5.35(0.07)[c]	5.11(0.07)[c]	4.09(0.19)[c]
	4.82(0.12)[d]	5.27(0.11)[d]	5.09(0.08)[d]	4.00(0.16)[d]
	4.72(0.01)[e]			
CH_2	4.16(0.23)[c]	4.02(0.13)[c]	4.16(0.07)[c]	≥2.38(0.06)[c]
CH_3	2.42(0.10)[c]	2.45(0.05)[c]	2.25(0.15)[c]	1.83(0.21)[c]
Si	2.51(0.11)	2.52(0.13)	2.87(0.10)	1.11(0.14)
SiH	2.33(0.11)	2.82(0.16)	2.76(0.25)	
SiH_2	2.17(0.08)	≥2.39(0.07)	≥2.39(0.07)	0.98(0.10)[f]
SiH_3	1.76(0.16)	2.13(0.16)	2.00(0.28)	

[a] Unless otherwise noted values are taken from the present study. Uncertainties of one standard deviation are listed in parentheses. Bond energies for MXH_x^+ (X = C or Si, x = 1−3) represent the energy difference between the ground state of this species (of unknown structure) and the theoretical dissociation products. [b] Reference 31. [c] This 0 K value has been converted from a 298 K value as described in ref 34. [d] Average value derived from previous and SiH_4 results, see text. [e] Reference 32. [f] There is a possibility that this value is ≥2.39 ± 0.07 eV, as discussed in the text.

A complication in understanding the trends in these bond energies is the possibility that some of the hydrogen atoms are bonded directly to the metal, e.g. $H-M^+-SiH_2$ instead of M^+-SiH_3, or that they bridge the metal and silicon atom. The first possibility cannot be ruled out entirely, although it seems unlikely because the metal−hydrogen bond energies (Table 4) are all weaker than even the weakest silicon−hydrogen bond, $D(H_2Si-H)$ = 2.95 eV (Table 2). Indeed, Ferhati and Ohanessian find that Y^+-SiH_2 is much more stable than $H-Y^+-SiH$.[12] Bridging hydrogens are known to be important in $Si_2H_4^+$, Si_2H_4, and Si_2H_2 species.[40-42] In the Si_2H_4 case, the ethane-like structure is calculated to be the ground-state structure but the double-bridged isomer, $HSi(H)_2SiH$, is a local minimum about 1 eV higher in energy. In the Si_2H_2 case, calculations indicate that the monobridged Si(H)SiH, disilavinylidene (H_2SiSi), and *trans*-HSiSiH isomers all lie within 0.9 eV of the ground-state double-bridged, $Si(H_2)Si$ structure. Consistent with this possibility is the theoretical finding of Ferhati and Ohanessian that the doubly-bridged $Y(H)_2Si^+$ structure has a comparable stability to the Y^+-SiH_2 structure.[12] The present results cannot be used to ascertain definitively which of the MH_xSi^+ structures or bonding mechanisms may be the most important, and it is possible that different structures of the products can be formed as the energy available to the system is increased.

Comparison with the Reactions of Sc^+, Y^+, La^+, and Lu^+ with Methane. To more clearly understand the effects that substitution of Si for C can have in organotransition metal bonding, we can compare our present results with those for the reactions of methane with Sc^+, Y^+, La^+, and Lu^+.[13] In general, the reactivities observed in the reactions with silane are quite similar to those observed for the reactions with methane. The lowest energy process observed in both systems is dehydrogenation to form $MXH_2^+ + H_2$ (X = Si or C). At higher energies, production of $MH^+ + XH_3$ dominates the reactivity. The only other product observed in the methane reactions is $MCH_3^+ + H$. No MC^+, MCH^+, or MH_2^+ products are observed.

The overall reactivity is greater in the silane systems than in the methane systems. At low energies in the SI data, the maximum observed cross section magnitudes for $MSiH_2^+$ are ~25, 110, 310, and 4 times larger than those for MCH_2^+ when M = Sc, Y, La, and Lu, respectively. At high energies, the total cross section magnitudes (largely MH^+ in both the silane and methane systems) are ~3, 1, 4, and 2.3 times larger for M = Sc, Y, La, and Lu, respectively. The increased contribution of MXH_2^+ in the silane systems relative to the methane systems may be explained by two factors. First, production of MXH_2^+ is thermodynamically more favorable in the silane systems because dehydrogenation of silane requires 2.39 eV while dehydrogenation of methane requires 4.71 eV. Second, previous work in our laboratory and others has demonstrated that hydrogen atom migrations are facile on silicon centers.[40,43,44] The increased hydrogen mobility at silicon centers could enhance the dehydrogenation process in the silane systems as compared to the methane systems.

Reaction Mechanism. The competition between the various product channels and the state-specific chemistry observed here is easily understood in terms of intermediate **I**, $H-M^+-SiH_3$, formed by inserting M^+ into a Si−H bond of silane. The analogous intermediate has been suggested for the reaction of Si^+ with SiH_4 and for M^+ with CH_4.[45-48] In addition, Ferhati and Ohanessian find **I** to be the key intermediate in their calculations of the $Y^+ + SiH_4$ reaction surfaces.[12] Although the structure of **I** is a reasonable choice for the reaction intermediate, consideration should also be given to the possibility that bridged isomers, e.g. $M^+(H)SiH_3$ or $M^+(H_2)SiH_2$, are involved instead. Such intermediates have also been postulated for the $Si^+ + SiH_4$ system,[47] but theoretical calculations of Raghavachari do not find these to be important.[48] Neither are they found to be important in the $Y^+ + SiH_4$ calculations.[12] The remainder of this discussion proceeds on the assumption that the primary intermediate has structure **I**, although the present results cannot be used to determine which of the MH_4Si^+ structures may be most important. This assumption is not meant to imply that different structures of the intermediates and products cannot be formed as the energy available to the system is increased. (It is useful to note that the qualitative ideas concerning the reaction mechanisms discussed below find parallels in the $Si^+ + SiH_4$ system,[46-48] although the quantitative aspects of these results are not directly applicable to the $MSiH_4^+$ systems because the two heavy atoms in this complex are different while they are identical in the $Si_2H_4^+$ system.)

There are two reasonable mechanisms for the dehydrogenation of **I** to form $MSiH_2^+$, which for M = Sc and Y has been calculated to have a singlet ground state.[10,12] The first possibility involves hydrogen migration to form intermediate **II**, $H_2M^+-SiH_2$, followed by reductive elimination of molecular hydrogen. Formation of this intermediate is indicated by the observation of the $MH_2^+ + SiH_2$ products. The intermediate analogous to **II** was discounted in the methane reactions because these divalent metal ions lack the electrons needed to covalently bond all three ligands. However, because of the decreased strength of the Si−H bonds, the greater mobility of hydrogen atoms on silicon centers,[40,43,44] and the ability of ground state SiH_2 ($^1A_1$)[49,50] to form a dative bond with the metal ions, intermediate **II** is a more reasonable possibility in the silane systems than in

(40) Boo, B. H.; Armentrout, P. B. *J. Am. Chem. Soc.* **1987**, *109*, 3549.
(41) Trinquier, G. *J. Am. Chem. Soc.* **1990**, *112*, 2130 and references therein.
(42) Grev, R. S.; Schaefer, H. F. *J. Chem. Phys.* **1992**, *97*, 7990.
(43) Kickel, B. L.; Fisher, E. R.; Armentrout, P. B. *J. Phys. Chem.* **1992**, *96*, 2603.
(44) Mandich, M. L.; Reents, W. D., Jr.; Jarrold, M. F. *J. Chem. Phys.* **1988**, *88*, 1703. Mandich, M. L.; Reents, W. D., Jr.; Kolenbrander, K. D. *J. Chem. Phys.* **1990**, *92*, 437.
(45) Armentrout, P. B. In *Gas Phase Chemistry*; Russell, D. H., Ed.; Plenum: New York, 1989; pp 1−41.
(46) The qualitative aspects of the reaction mechanism for $Si^+ + SiH_4$ were first examined by Boo and Armentrout.[47] Subsequent calculations of Raghavachari[48] elucidated the most important pathways and intermediates.
(47) Boo, B. H.; Armentrout, P. B. *J. Am. Chem. Soc.* **1987**, *109*, 3549.
(48) Raghavachari, K. *J. Chem. Phys.* **1988**, *88*, 1688.
(49) Berkowitz, J.; Greene, J. P.; Cho, H. *J. Chem. Phys.* **1987**, *86*, 1235.
(50) Bauschlicher, C. W.; Taylor, P. R. *J. Chem. Phys.* **1987**, *86*, 1420.

methane systems. The second possibility is a four-centered elimination of molecular hydrogen from **I**, which should be considered for two reasons. First, for the reactions of methane with Sc^+, Y^+, La^+, and Lu^+,[13] we concluded that formation of $MCH_2^+ + H_2$ occurred via a four-centered elimination. Second, theoretical calculations suggest that a four-centered elimination can occur with little or no barrier if the metal−ligand bonds are covalent and have substantial d character.[51] Ferhati and Ohanessian considered both of these mechanisms and found that the four-centered elimination provided the lowest energy pathway and formed the Y^+-SiH_2 structure.[12]

The observed competition between MH^+, MH_2^+, and $MSiH_2^+$ in reactions 4, 5, and 8, respectively, may be explained in terms of a common intermediate **I** which can dissociate to form $MH^+ + SiH_3$, lose H_2 via a four-centered elimination, or transfer a hydrogen to form **II**. Intermediate **II** decomposes by breaking the M^+-Si bond to form $MH_2^+ + SiH_2$ or by reductive elimination of H_2 to form $MSiH_2^+ + H_2$. The observation that the cross section magnitudes for MH^+ and MH_2^+ are within a factor of ~2 for M = Y, La, and Lu suggests that rearrangement of **I** to form **II** is facile. The same is not true for M = Sc, where the $MH_2^+ + SiH_2$ cross section is not observed for reaction of ground state Sc^+ (a^3D) and is about 50 times smaller than that for $MH^+ + SiH_3$ for reaction of Sc^+ (a^1D, a^3F). Other higher energy decomposition pathways available to intermediate **I** include dissociation by simple bond cleavage to form $MSiH_3^+ + H$ and $MH^+ + SiH_3$. As discussed above, decomposition of $MSiH_3^+$ and $MSiH_2^+$ occurs by dehydrogenation to form $MSiH^+ + H_2$ and $MSi^+ + H_2$, respectively.

Molecular Orbital and Spin Conservation. As in the methane reaction systems,[13] the interaction of individual electronic states with silane may be understood by using simple molecular orbital arguments. Oxidative addition of a Si−H bond to a metal center can be achieved by donation of the bonding σ electrons into empty ns or $(n-1)d\sigma$ orbitals of the metal and back-donation of metal $(n-1)d\pi$ electrons into the σ^* antibonding orbital. This serves to increase the electron density between the metal and the molecular fragment and lengthen the Si−H bond. Furthermore, this simple idea would predict that states having an occupied ns or $(n-1)d\sigma$ orbital will have repulsive interactions with the Si−H bonding σ electrons.

Spin conservation is another factor that needs to be considered in the reactivity of metal ions and can be used to understand the observed electronic state effects. Reactions 10−15 show the spin states of the individual species for the observed reactions where the number in parentheses is the spin quantum number of that particular species. The indicated spin states for SiH_4, SiH_2, H_2, and H are known.[39,49,50,52] The ground states of MH^+ have been calculated or suggested to be doublets.[31,35,53] The spins of the ground states for $ScSiH_2^+$, $YSiH_2^+$, and ScH_2^+ have been calculated to be singlets.[10,12,54] We assume that the ground spin states for $MSiH_2^+$ and MH_2^+ (M = Y, La, and Lu) are also singlets. We assume that $MSiH_3^+$ has a single M−Si covalent bond and therefore has the same spin state as MH^+. The spins are assumed to be the same for $MSiH^+$ and MSi^+ as their precursors, $MSiH_3^+$ and $MSiH_2^+$, respectively. This is indicated by the observed efficiencies for the dehydrogenation of the latter ions.

$$M^+(1,0) + SiH_4(0) \longrightarrow MH^+(^1/_2) + SiH_3(^1/_2) \quad (10)$$
$$\longrightarrow MH_2^+(0) + SiH_2(0) \quad (11)$$
$$\longrightarrow MSi^+(0) + 2\,H_2(0) \quad (12)$$
$$\longrightarrow MSiH^+(^1/_2) + H_2(0) + H(^1/_2) \quad (13)$$
$$\longrightarrow MSiH_2^+(0) + H_2(0) \quad (14)$$
$$\longrightarrow MSiH_3^+(^1/_2) + H(^1/_2) \quad (15)$$

Therefore, reactions 11, 12, and 14 are spin-allowed for low-spin singlet, but not high-spin triplet states of M^+. This is consistent with the large enhancement observed for the reactions of Y^+ (a^1S) and is a further argument for believing that the Sc^+ (a^1D, a^3F) cross sections can be attributed largely to the a^1D state. The observation that the a^3D high-spin states undergo reactions 11 (except Sc^+), 12, and 14 implies that spin−orbit coupling exists between high- and low-spin state surfaces. The relatively inefficient reactivity of the high-spin states compared to the low-spin states of Sc^+ and Y^+ implies that this coupling is rather poor. As discussed above, the shapes of the $YSiH_2^+$ cross sections are different for the state-specific reactions of Y^+ (a^1S) and Y^+ (a^3D). The $E^{-1/2}$ decline in the $YSiH_2^+$ cross section for the a^1S ground state reaction is that expected for an exothermic ion−molecule reaction;[55] however, the $YSiH_2^+$ cross section for the a^3D excited state reaction declines as $\sim E^{-1.4\pm0.2}$. The difference in the energy dependence of these two cross sections implies that there is an energy dependence associated with the coupling between the high- and low-spin surfaces. An energy dependence close to E^{-1} has been observed previously[56] and can be understood in terms of a Landau−Zener type of formalism.[57,58] In the case of La^+, we observe no changes in reactivity for ions generated in the DC/FT and SI sources, an obvious result if the electronic temperature generated in the DC/FT source is comparable to that from the SI source. If, however, the DC/FT source yields nearly thermal room temperature ions (as for Sc^+ and Y^+), then this result indicates that the La^+ (a^1D) first excited state is not substantially more reactive than the La^+ (a^3F) ground state. This observation can be rationalized if the spin−orbit coupling between the high- and low-spin surfaces is fairly efficient in this case, which seems reasonable for such a heavy metal.

Reactions 10, 13, and 15 are spin-allowed from both high- and low-spin states of M^+. This could help to explain our difficulty in establishing reliable state-specific $ScSiH^+$ and $ScSiH_3^+$ cross sections. Because production of these species is allowed from both spin states of Sc^+ and the cross sections are relatively small, it is difficult to observe a change in reactivity when low-spin states are present. The same is true for Y^+. The production of $YSiH_3^+$ and $YSiH^+$ is not significantly enhanced for low-spin states relative to that for high-spin states. In contrast, the ScH^+ and YH^+ cross sections show large enhancements for reaction of low-spin M^+ states. As noted above, the MH^+ (as well as the MH_2^+) products compete with $MSiH_2^+$ formation, indicating that a common intermediate to these processes is involved. If this intermediate has a low-spin ground state, e.g., as would be likely for intermediate **I** if both bonds to the metal are covalent, then the low-spin-state enhancement is easily explained. Formation of **I** occurs diabatically from states having the correct spin and electronic configuration. The lowest states that meet these requirements

(51) Stelgerwald, M. L.; Goddard, W. A., III *J. Am. Chem. Soc.* **1984**, *106*, 308. Rappe, A. K. *Organometallics* **1987**, *6*, 354.
(52) Chase, M. W.; Davies, C. A.; Downey, J. R., Jr.; Frurip, D. J.; McDonald, R. A.; Syverud, A. N. *J. Phys. Chem. Ref. Data* **1985**, *14*, Supp. No. 1 (JANAF Tables).
(53) Petterson, L. G. M.; Bauschlicher, C. W.; Langhoff, S. R.; Partridge, H. *J. Chem. Phys.* **1987**, *87*, 481.
(54) Rappe, A. K.; Upton, T. H. *J. Chem. Phys.* **1986**, *85*, 4400.
(55) Gioumousis, G.; Stevenson, D. P. *J. Chem. Phys.* **1958**, *29*, 292.
(56) Burley, J. D.; Ervin, K. M.; Armentrout, P. B. *J. Chem. Phys.* **1987**, *86*, 1944.
(57) Landau, L. D. *Phys. Z. Sowjetunion* **1932**, *2*, 46.
(58) Zener, C. *Proc. R. Soc. London Ser. A* **1975**, *137*, 696.

are the b^1D [$(n-1)d^2$] states for all four metal ions. For Sc^+, the attractive surface derived from the b^1D state will undergo an avoided crossing with the somewhat more repulsive a^1D (3d4s) state, such that the a^1D state adiabatically correlates with insertion. For Y^+, there will also be an avoided surface crossing between the surface evolving from the a^1S ($5s^2$) state, which should be even more repulsive due to the doubly occupied 5s orbital, and that evolving from the a^1D (4d5s) state. The surface evolving from the Sc^+ (a^3D, 3d4s) state should also be relatively repulsive and must cross the singlet surface leading to the insertion intermediate. The extent to which these surfaces mix will dictate the reaction efficiency of the a^3D state. Similar situations occur for Y^+ and La^+, where the a^3D and a^3F states, respectively, presumably react via a triplet–singlet surface interaction. As mentioned above, this crossing is expected to be more efficient for the heavier metals because of enhanced spin–orbit coupling.

Efficient spin–orbit coupling may also explain why Lu^+ (a^1S) is observed to react with reasonable efficiency. We would expect that the a^1S ($6s^2$) electron configuration would lead to a fairly repulsive potential energy surface. Because the a^1D (5d6s with some $5d^2$ character) and b^1D ($5d^2$) states of Lu^+ lie well above the a^1S ($6s^2$) ground state, by 2.15 and about 4.5 eV, respectively,[26] the surface that diabatically leads to intermediate **I** should be much less accessible from the Lu^+ ground state reactants than for the other metal systems. However, efficient spin–orbit coupling probably allows the repulsive surface evolving from Lu^+ (a^1S) to interact with those evolving from the a^3D (5d6s) first excited state and the a^3F ($5d^2$) state, which lie about 1.5 and 3.6 eV higher in energy. These excitation energies are still well above those for Y^+ and La^+ which probably explains why Lu^+ is less reactive than these metals at the lowest energies.

Summary

In this study, we investigate the reactions of silane with Sc^+, Y^+, La^+, and Lu^+. We observe formation of MH^+, MH_2^+, and $MSiH_x^+$ ($x = 0-3$) species. Threshold analyses of the cross sections allow the determination of 0 K bond dissociation energies for M^+-SiH_x ($x = 0-3$). In agreement with theoretical predictions,[10] the Sc^+-SiH_2 bond is weaker than the Sc^+-CH_2 bond, a result also obtained for the other M^+-SiH_2 (M = Y, La, and Lu) vs M^+-CH_2 species. Trends in metal–silicon bond energies are discussed, although a definitive understanding of these trends is complicated because the most important structures for the $MSiH_x^+$ species cannot be determined from the present results.

We observe that the reactions of the low-spin Sc^+ (a^1D) and Y^+ (a^1S) states are more efficient than those of the high-spin Sc^+ (a^3D) and Y^+ (a^3D) states. Indeed, formation of ScH_2^+ is observed to occur only in the reaction of silane with the Sc^+ (a^1D) excited state. These results suggest the existence of low-spin-state intermediates that we discuss in terms of $H-M^+-SiH_3$ structures, consistent with the theoretical conclusions of Ferhati and Ohanessian,[12] although hydrogen-bridged isomers may also be involved. The observation of $MH_2^+ + SiH_2$ products suggests that a second intermediate with the $H_2M^+-SiH_2$ structure is also formed. High-spin triplet states of these metal ions are observed to undergo spin-forbidden reactions indicating that spin–orbit coupling between high- and low-spin surfaces is important. Such coupling appears to be fairly efficient for the heavy metals, La^+ and Lu^+.

Acknowledgment. This work was supported by the National Science Foundation under Grant CHE-9221241. We thank Prof. S. Geribaldi for bringing these reactions to our attention.

JA943281H